Journal of King Saud University - Science 35 (2023) 102971

HOSTED BY

Contents lists available at ScienceDirect

Journal of King Saud University - Science

journal homepage: www.sciencedirect.com

Spectroscopic studies on the antioxidant and anti-tyrosinase activities of anthraquinone derivatives

Velmurugan Loganathan [a], Idhayadhulla Akbar [a,*], Mohammad Z. Ahmed [b], Shadab Kazmi [c], Gurusamy Raman [d]

[a] Research Department of Chemistry, Nehru Memorial College (Affiliated Bharathidasan University), Puthanampatti-621007, Tamil Nadu, India
[b] Department of Pharmacognosy, College of Pharmacy, King Saud University, P.O. Box 2455, Riyadh 11451, Saudi Arabia
[c] Department of Child Health, School of Medicine, University of Missouri, Columbia, MO, USA
[d] Department of Life Science, Yeungnam University, Gyeongsan, Gyeongbuk-do 38541, South Korea

ARTICLE INFO

Keywords:
Anthraquinone
Antioxidant activity
Anti-tyrosinase activity
Molecular docking

ABSTRACT

Objectives: Anthraquinones (9,10-dioxoantracenes) with a wide range of applications constitute an important class of natural and synthetic compounds. Moreover, there is an increasing interest in developing new anthraquinone derivatives with biological activity. These findings suggested that due to the qualities of anthraquinone, it may be employed in the pharmaceutical and food industries.

Methods: The synthesis of anthraquinone derivatives (**compound 1** and **2**) was performed using the Mannich base reaction, and the compounds were characterised via FT-IR, ^{1}H and ^{13}C NMR spectra, and mass spectral analysis. Through the use of spectroscopic analytical techniques, the *in vitro* antioxidant capacity of anthraquinone was examined. These techniques included DPPH free radical scavenging, hydrogen peroxide (H_2O_2) scavenging, $ABTS^{\bullet+}$ scavenging activity, ferrous ion (Fe^{2+}).

Results: At a concentration of 100 μg/mL, **compound 2** shows that 65.2 % inhibited to DPPH assays compared with butylated hydroxyl toluene (BHT) at 45.7 % activity. Moreover, **compound 2** shows that more potential of activity against DPPH, $ABTS^{\bullet+}$, hydrogen peroxide, ferric ion (Fe^{3+}), and ferrous ion (Fe^{2+}) chelating, reducing, and antioxidant properties when compared with **compound 1** and standard BHT. The **compounds 1** and **2** where checked for tyrosinase activity, the **compound 2** shows that significant of activity compared with **compound 1** and standard kojic acid.

Conclusion: Kinetics studies were analysed **compounds 1** and **2** through all antioxidant assays and activity of tyrosinase inhibition. The **compound 2** was highly active against all the activities. Based on the aforementioned findings, it can be used to maintain nutritional quality, extend the shelf life of food and medicine, delay the development of hazardous oxidation products, and minimise or stop the oxidation of lipids in dietary items.

1. Introduction

Several living things receive energy from oxidation for a variety of metabolic functions. Proper body production of free radicals and the number of antiradicals needed to squelch them and shield the body from their damaging effects are in balance. At the cellular level, oxidative damage is mostly caused by free radicals like superoxide anion, H_2O_2 and OH radicals (Diep et al., 2022; Ighodaro and Akinloye, 2018). Reactive oxygen species (ROS) induced biochemical reaction alterations are increasingly being implicated as causative agents in a number of chronic human diseases, including diabetes, cancer, atherosclerosis, inflammation, rheumatoid arthritis, and neuron degeneration (Juan et al., 2021). Human body has developed many mechanisms both enzymatic and nonenzymatic to eliminate reactive oxygen species (ROS) but not enough to combat in severe oxidative stress conditions (Garcia-Caparros et al., 2021). To find out how to stop oxidative diseases from developing, numerous studies have been conducted. The most researched method for preventing oxidative stress is to increase the body's natural antioxidant levels, which can be done by eating more fruits and vegetables.

Peer review under responsibility of King Saud University.
* Corresponding author.
E-mail address: a.idhayadhulla@gmail.com (I. Akbar).

https://doi.org/10.1016/j.jksus.2023.102971
Received 8 April 2023; Received in revised form 17 September 2023; Accepted 25 October 2023
Available online 27 October 2023

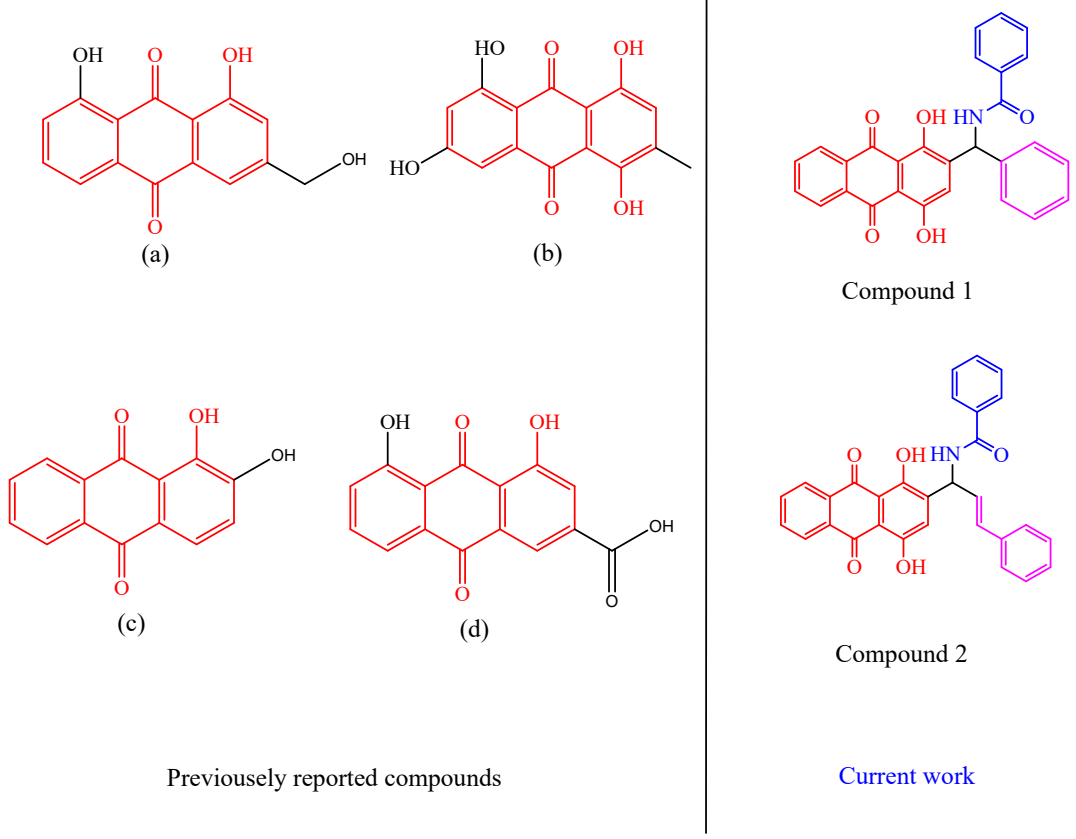

Fig. 1. Some previously reported compounds.

Natural antioxidants, especially polyphenolic, are risk-free and have been shown to have biological and pharmacological effects. Because of this, in-depth investigation has been conducted recently to identify which plants have anti-radical abilities that could be consumed by humans (Berretta et al., 2020). The study of medicine nowadays is focused on developing plant-based treatments for illnesses brought on by oxidative stress. Fresh fruit, vegetables, and antioxidant-rich tea consumption have been associated with a decreased risk of cancer and heart disease (Maher, 2020). There is a correlation between increased plant food consumption and a decreased danger of death from these conditions of the anti-tumour and anti-infective medicines that are commercially accessible, around 60 % are natural (Wang et al., 2022). The main component of plants responsible for their antioxidant capabilities is polyphenol. The redox capabilities of polyphenols, by virtue of which they can act as hydrogen donors, metal cheaters, singlet oxygen quenchers, reducing agents, and reluctant of ferritin haemoglobin, are primarily responsible for their antiradical effects (Assefa et al., 2018; Karim et al., 2020).

Anthracene displays the aromatic compound with two keto functionalities at the 9-and 10-positions (Malik, 2016). Because the planar anthraquinone core can be embedded in the DNA (Deoxyribonucleic acid) double helix in cancer cells and go through a particular redox cycle that produces the superoxide radical anion ($O_2^{\bullet+}$) in vivo, the function of the anthraquinone scaffold has attracted the attention of medicinal chemists (Tian et al., 2020). With numerous uses, anthraquinones (9,10-dioxoantracenes) are a significant family of both natural and artificial substances. Additionally, creating novel anthraquinone compounds with biological action is becoming more popular (Cicek et al., 2019). Anthraquinones have an extensive variety of pharmacological effects, including anti-HIV, cytotoxic, and anti-plasmodia actions (Feilcke et al., 2019), and antifungal, antibacterial, and antiviral effects (Mohamadzadeh et al., 2020). Anti-platelet, anti-coagulant, anti-malarial, and then anti-tubercular effects, neuroprotective and anti-inflammatory effects, and activity against multiple sclerosis (Chighizola et al., 2018; Dehnavi et al., 2021; Rastogi et al., 2019; Kammona, and Kiparissides, 2020). According to the structure of the maternal nucleus, anthraquinones are typically split into the monomers of anthraquinone, which can then be further separated into hydroxyanthraquinones, bianthraquinones, anthranones, and anthranols (Liu et al., 2016). Anthraquinones are one of the numerous secondary metabolites made by different plants. They are used in a broad range of sectors, such as the culinary and fibre industries, as well as in medicine to treat a variety of illnesses (Tikhomirov et al., 2018). They come from the compound 9,10-anthracenedione. Different anthraquinone compounds, which have a wide range of therapeutic characteristics, are formed when 9,10-anthracenedione is modified with –OH, CH_3, –COOH, $–OCH_3$ (hydroxyl, methyl, carboxyl and methoxy groups) . Anthraquinones, a class of chemical compounds, have numerous biological activities, including possible industrial uses. The bulk of them are produced by living things, mostly plants and microbes (Duval et al., 2016). Fittig first suggested the right di ketone structure of anthraquinones in 1873, which is still commonly used today (Malik et al., 2021). Since then, lichens, marine sources, fungi, and various types of medicinal plants have all been shown to contain more than 75 naturally occurring anthraquinones (Masi and Evidente, 2020; Vitale et al., 2020).

In an effort to support complementary therapies, researchers have recently been attempting to extract antioxidants from herbal sources. The antioxidant capacity of *G. aparine* (*Galium aparine* species) has been mentioned in a few early publications, butthe whole flavonoid its precise scavenging and decreasing ability, total flavonoid concentration, then phenolic content in various fractions have not been mentioned (Korkmaz et al., 2021; Friščićet al., 2018; Özmatara, 2020). Some previously reported anthraquinone derivative shown in Fig. 1(Siddamurthi et al., 2020′ Martorell et al., 2021; Gecibesler et al., 2021). The most potent

antioxidant fraction can be supplemented by the varying levels of phytochemicals' solvent solubility with varying polarities. This study's primary goals were to assess antioxidant activity, anti-tyrosinase activity, and radical scavenging activities in different anthraquinone derivatives by a spectroscopic method. The newly synthesised anthraquinone derivative findings suggested that due to the qualities of anthraquinone, it may be employed in the pharmaceutical and food industries.

2. Experimental

2.1. Chemicals

All chemicals were purchased from Sigma Chemicals Co. in St. Louis, Missouri, USA. These materials were of analytical quality. From Merck, we obtained H_2SO_4, beta-D-2-deoxyribose, Na_2CO_3, NaOH, $NaNO_2$, Na_2HPO_4, NaH_2PO_4, H_2O_2, $FeCl_2$, and $K_4[Fe(CN)_6]$. $3H_2O$. A Nicolet iS5 FTIR (4000–400 cm^{-1}) from Thermo scientific was used to analyze all substances. On a Bruker DRX-300 MHz, 75 MHz, we conducted NMR spectroscopy analysis on the ^1H and ^{13}C. Using an elemental analyser (Model Varioel III), the amounts of C, H, S, and N were determined. Mass spectra were recorded by PerkinElmer GCMS model Clarus sq8 (EI).

2.2. N-((1,4-dihydroxy-9,10-dioxo-9,10-dihydroanthracen-2-yl)(phenyl)methyl)benzamide

2.2.1. Synthesis of compound 1

To mixture of 1,4-dihydroxyanthracene-9,10-dione (0.01 mmol of 2.40 g), benzamide (0.01 mmol of 1.21 g), and benzaldehyde (0.01 mmol of 1.02 mL) were added in ethanol (10 mL) at reflux 1 h at 60 °C. The obtained solid material was washed with water. The final product was identified and conformed by using thin-layer chromatography. The solid substance is separated using column chromatography with ethyl acetate and hexane (4:3 ratio).

Yellow solid; yield 87 %; mp: 165–169 ^{0}C; IR (KBr, cm^{-1}): 3359 (NH), 1765 (CO), 3353 (–OH). ^1H NMR (DMSO-d_6), δ(ppm): 8.29–7.88 (4H, dd, Ar-CO ring), 8.03 (–NH, 1H, s), 8.03–7.63 (Ar-ring, 5H, m), 7.37–7.26 (Ph-ring, 5H, m), 7.09 (=CH, 5H, m), 6.16 (NH-CH, 5H, m), 5.35 (2-OH, 5H, m); ^{13}C NMR (DMSO-d_6), δ(ppm): 187.1 (1C, CO), 186.9 (1C, C = O), 166.1 (1C, CO), 155.0, 153.44, 124.3, 118.7, 116.6, 112.2 (6C, Hq-ring), 141.3, 129.2, 128.2, 126.2 (6C, Ph-ring), 134.2, 132.1, 128.8, 127.5 (6C, Ar-CO ring), 133.6, 132.1, 126.8 (6C, Ar-ring), 51.6 (1C, NH-C). EI-Ms, *m/z* (Relative intensity %): 449.13 (M^+, 30.7 %). Anal. Cacld. $C_{28}H_{19}NO_5$: C, 74.83; H, 4.25; N, 3.11, Found: C, 74.85; H, 4.26; N, 3.13 %.

2.3. (E)-N-(1-(1,4-dihydroxy-9,10-dioxo-9,10-dihydroanthracen-2-yl)-3-phenylallyl) benzamide

2.3.1. Synthesis of compound 2

To mixture of 1,4-dihydroxyanthracene-9,10-dione (0.01 mmol of 2.40 g), benzamide (0.01 mmol of 1.21 g), and cinnamaldehyde (0.01 mmol of 1.25 mL) were added in ethanol (10 mL) at reflux 1 h at 60 °C. The obtained solid material was washed with water. The final product was identified and conformed by using thin-layer chromatography. The solid substance is separated using column chromatography with ethyl acetate and hexane (4:3 ratio).

Yellow solid; yield 84 %; mp: 172–174 ^{0}C; IR (KBr, cm^{-1}): 3495 (NH), 1860 (CO), 3540 (–OH). ^1H NMR (DMSO-d_6), δ(ppm): 8.29–7.88 (Ar-CO ring, 4H, dd), 8.03 (–NH, 4H, dd), 8.03–7.63 (Ar-ring, 4H, dd), 7.40–7.24 (Ph-ring, 4H, dd), 7.09 (=CH, 4H, dd), 6.66 (–CH, 1H, s), 6.37 (Ph-CH, 1H, s), 5.56 (NH-CH, 1H, s), 5.35 (2-OH, 1H, s); ^{13}C NMR (DMSO-d_6), δ(ppm): 187.1 (1C, CO), 186.9 (1C, C = O), 167.8 (1C, CO), 154.3, 152.1, 127.6, 117.4, 115.9, 112.7 (6C, Hq-ring), 136.4, 128.6, 128.5, 127.9 (6C, Ph-ring), 134.2, 132.1, 128.8, 127.5 (6C, Ar-CO ring), 133.6, 132.1, 126.8 (6C, Ar-ring), 129.5 (1C, Ph-C), 123.3 (1C, =C-), 52.4 (1C, NH-C). EI-Ms, *m/z* (Relative intensity %): 475.14 (M^+, 32.9 %). Anal. $C_{30}H_{21}NO_5$: C, 75.78; H, 4.43; N, 2.95, found: C, 75.75; H, 4.45; N, 2.93 %.

2.4. Antioxidant assays

2.4.1. DPPH free radical scavenger assay

The vivid purple type and absorption at 517 nm of **compounds 1** and **2** against DPPH assays. As a result, anti-radical activity and the amount of leftover DPPH are inversely associated. Several quantities of the test compounds (varying from 25 to 100 μg/mL in methanol) were added to a 0.004 % solution in 4 mL (w/v) methanolic solution of DPPH. The absorbance at 517 nm was measured against a blank after a 30-minute incubation period at room temperature (Kumar et al., 2017).

To calculate the percentage of free radical scavenging (%), the following equation was used:

$$Scavenging\%DPPHScavengingeffect(\%) = \frac{A_{control} - A_{sample}}{A_{control}} \times 100$$

Where,

A_{sample} represents the measured material's absorbance and $A_{control}$ represents the DPPH solution's absorbance, which contains all of the reagents other than the test substance. There were three runs of each test.

2.5. Fluorescence spectroscopy analyze of scavenging hydroxyl radicals (OH· Scavenging activity)

2.5.1. Method for hydroxylating benzoic acid

The Fenton reaction, which produces –OH at the C_3 or C_4 position of the benzene ring, converts benzoic acid into hydroxyl. $FeSO_4$ (10 mmol), $7H_2O$ (10 mmol), EDTA (10 mmol), and the representative solution were combined in 0.2 mL in a test tube with a screw top. The sample solution, phosphate buffer (pH 7.4, 0.1 mol), and 0.2 mL of sodium benzoate (10 mmol) were then mixed together to get a final volume of 1.8 mL. Finally, 0.2 mL of a 10 mmol H_2O_2 solution was added, and the combination was pre-incubated for 2 h at 37 °C using BHT as the standard for excitation following this incubation, fluorescence was assessed at 407 nm release (305 nm).

$$OHradicalscavengingactivity = \left(1 - \frac{F.I._{.s} - F.I._{.o}}{F.I._{.c} - F.I._{.o}}\right) \times 100$$

Where,

Fluorescence intensity at 305 and 407 nm without treatment, or $F.I._{O.}$ $F.I._{C.}$ stands for fluorescence intensity for the treatment control at 305 and 407 nm. Fluorescence intensity of the treated sample at 305 and 407 nm (Wang et al., 2022).

2.5.2. Activation of hydrogen peroxide scavengers (H_2O_2 Scavenging activity)

The calculation of the H_2O_2 scavenging capacity is explained by Lateef (Lateef et al., 2017). In brief, an H_2O_2 solution with a 40 mM concentration was produced using phosphate buffer (pH 7.4). The H_2O_2 solution was subsequently exposed to test substances at concentrations between 25 and 100 μg/mL. At 230 nm, the absorbance values of the reaction mixture were calculated. To calculate the percentages of H_2O_2 scavenging, use the equation below. Percent scavenging $A_{control}$ A_{sample} = 100 $A_{control}$ where A_{sample} denotes the absorbance of the test compounds and $A_{control}$ denotes the absorbance of the control reaction, which uses all reagents other than the test compound. Each test was done three times.

$$IC_{50}Inhibition = \frac{A_{control} - A_{sample}}{A_{sample}} \times 100$$

Where,

A_{sample} is the test substances' absorbance, and $A_{control}$ is the

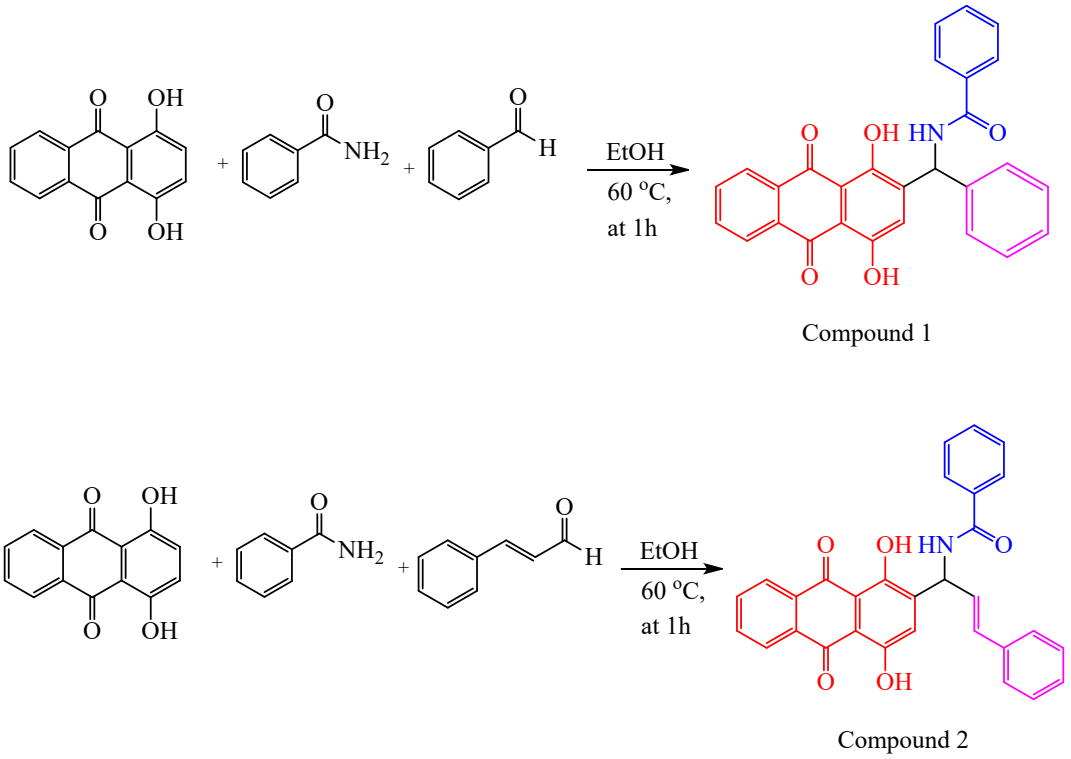

Scheme 1. Synthesis of route of compound 1 and 2.

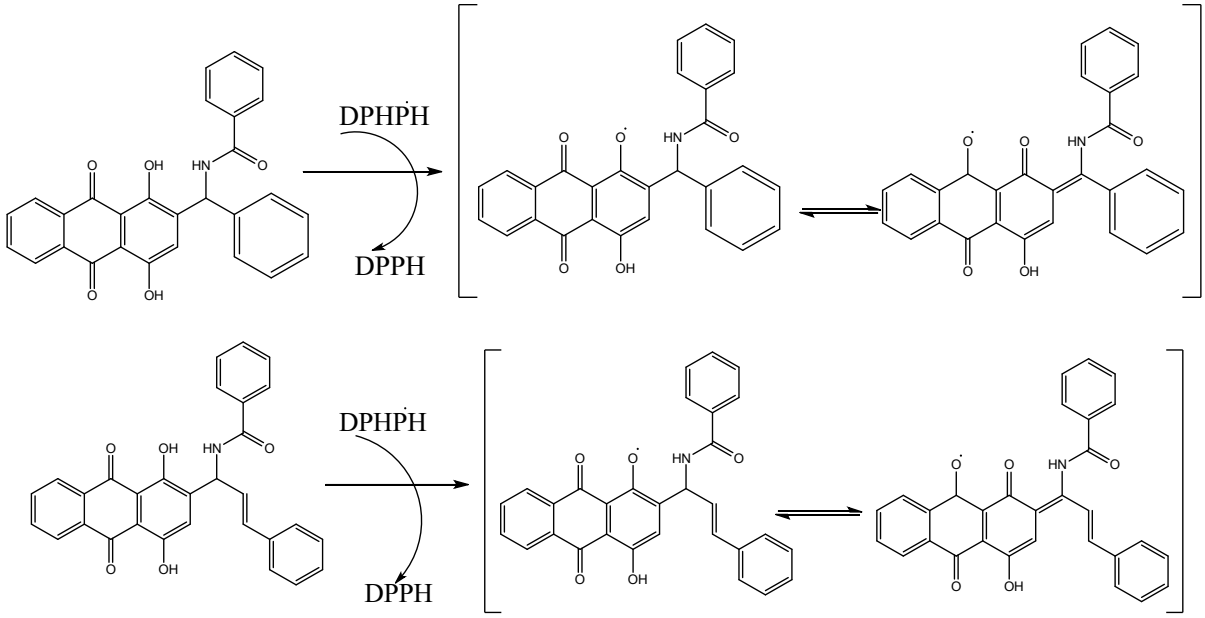

Scheme 2. Compounds 1 and **2** DPPH radicals scavenging activity.

absorbance of the control reaction (which contains all reagents but the test compound).

2.5.3. Activity for scavenging nitric oxide (NO· Scavenging activity)

With a few minor adjustments, the measurement of nitric oxide scavenging activity adhered to the standards set by Ghosh (Ghosh and Tiwari, 2018). NO· were created by the reaction of sodium nitroprusside. The test chemicals (**1** and **2**) were introduced in various concentrations (range from 25 to 100 μg/mL) and incubated for 150 min at 258 °C with $C_5FeN_6Na_2O$ (10 mM, 1 mL) and 1.5 mL of phosphate buffer saline (0.2 M, pH 7.4). The reaction mixture was added to the Griess reagent after it had been incubating for 1 mL (1 % sulphanilamide, 2 % H_3PO_4, and 0.1 % naphthylethylenediaminedihydrochloride). The chromosphere absorption was measured at 546 nm. The nitric oxide scavenging activity was calculated using the following equation.

$$\%NOScavenging = \frac{A_{control} - A_{sample}}{A_{control}} \times 100$$

Where, $A_{control}$ represents the absorbance of the control reaction and A_{sample} represents the absorbance of the test chemicals (which contains

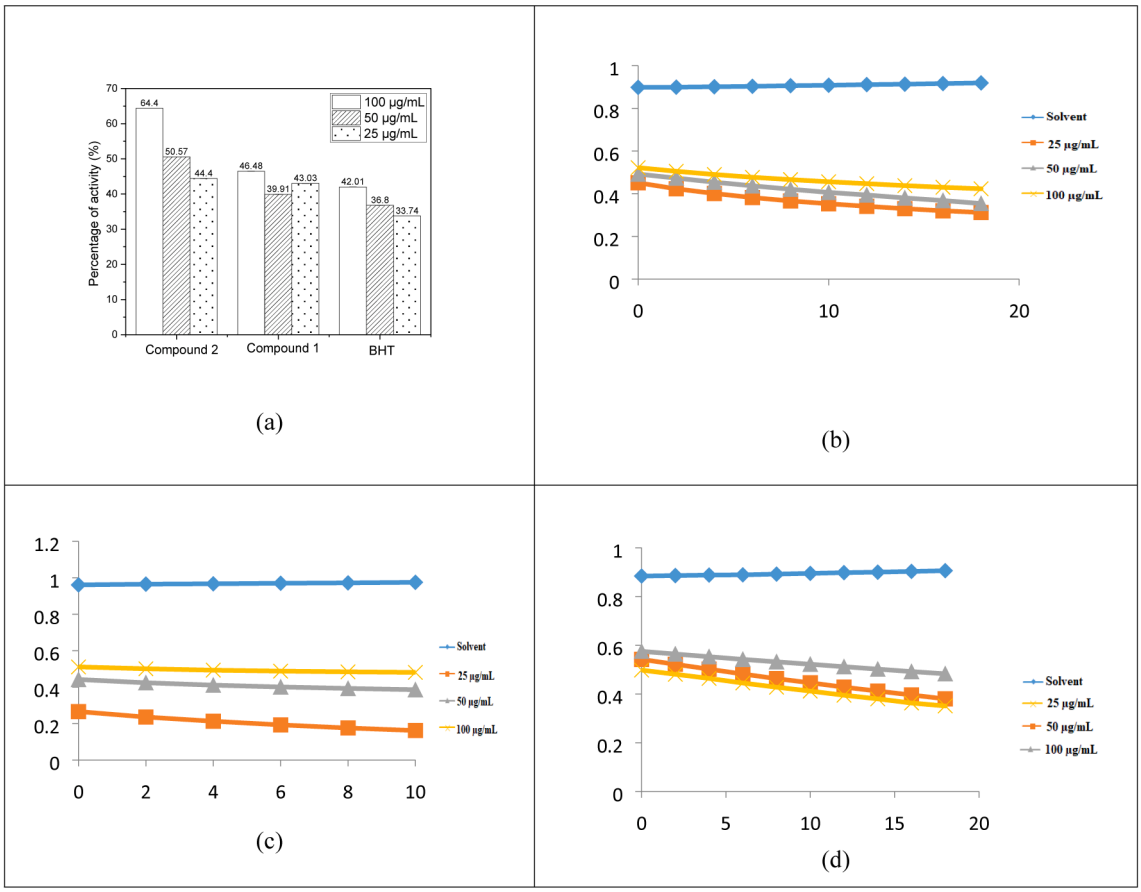

Fig. 2. Percentage of activity of compounds **1,2,** and **BHT** DPPH assays (a), compound **1** DPPH kinetics (b), compound **2** DPPH kinetics (c), and BHT DPPH kinetics (d).

all reagents but the test compound.

2.5.4. Ferric reducing antioxidant power (FRAP) assay

Using the previously described technique, the FRAP test was carried out by Benzie and Strain. Freshly prepared FRAP reagent was created by mixing 2.5 mL of TPTZ (10 mM), 40 mM HCl, 20 mL of $FeCl_3$, and 25 mL of acetate buffer (300 mM concentration and pH 3.6). The presence of Fe^{2+}-TPTZ in the light blue reagent indicates that Fe^{3+}-TPTZ is present, which changes to dark blue when it interacts with antioxidants. The increase in absorbance seen at different concentrations of the **compounds** (**1** and **2**) in FRAP reagent (100, 50, and 25 µg/ml) at a wavelength of 593 nm was the cause of these modifications (Benzie and Devaki, 2018).

2.5.5. Anti-tyrosinase activity

All of the compounds were put through an inhibition of tyrosinase test with L-DOPA as the substrate for purpose of evaluating the tyrosinase inhibition, in accordance with the method described by Bradford with a few minor modifications (Selvaraj et al., 2020). As a result, the reference ingredient was chosen to be kojic acid, a substance that is frequently used to whiten the skin due to its significant inhibitory activity against tyrosinase.

2.5.6. Molecular docking analysis

The most potent anthraquinone series **compounds** (**1** and **2**) and the proteins 2Y9X were subjected to molecular docking investigations using Auto Dock Vina 1.1.2 to examine the mechanism of binding and interactions (Chidambaram et al., 2021). The collected data were then assessed in relation to the molecular docking models of the reference medications, which comprised Kojic acid. The **Compounds 1, 2**, and Kojic acid all have three-dimensional models made using the Chem Draw Ultra 12.0 application.

3. Results and discussion

3.1. Chemistry

Here, the usual technique was used to synthesize anthraquinone derivative **compounds 1** and **2**. A mixture of 1,4-dihydroxyanthracene-9,10-dione, 3-carbamoylbenzene-1-ylium, and benzaldehyde combined with ethanol under the reflux method for 1 h at 60 °C. The final product was identified and conformed by using TLC and separated by column chromatography. The synthetic route outline is shown in scheme 1. The product yield was 87–84 %.

The generated compounds were described using IR, ^{1}H, ^{13}C, and mass spectrometry techniques. The NH, CO, and –OH were matched by each compound, and bands in the IR that are distinctive to **compounds 1** and **2** had substantial regions of absorption at 3495–3359, 1860–1765, and 3540–3353 cm^{-1}, respectively. The ^{1}H NMR signal ranged from 8.03 to 7.63, 7.40–7.26, 5.35, and 8.03 ppm, corresponding to the protons Ar-ring, -Ph-ring, –OH, and NH. The ^{13}C NMR revealed signals that corresponded to the -C = O, –NH-C, Ar-ring, and Ph-ring atoms at ppm values of 187.1–166.1, 52.4–51.6, 133.6–126.8, and 141.3–126.2. Elemental analysis and mass spectroscopy were checked and confirmed the compounds structure. The molecular weight was determined by mass spectral characterization (EI-MS), the **compound 1a** shows that molecular ions EI-MS (*m/z*):449.13 (M^{+}, 30.7 %) peak confirmed by the molecular weight of **compound 1**. All compounds were conformed the molecular mass using EI-MS mass spectral analysis.

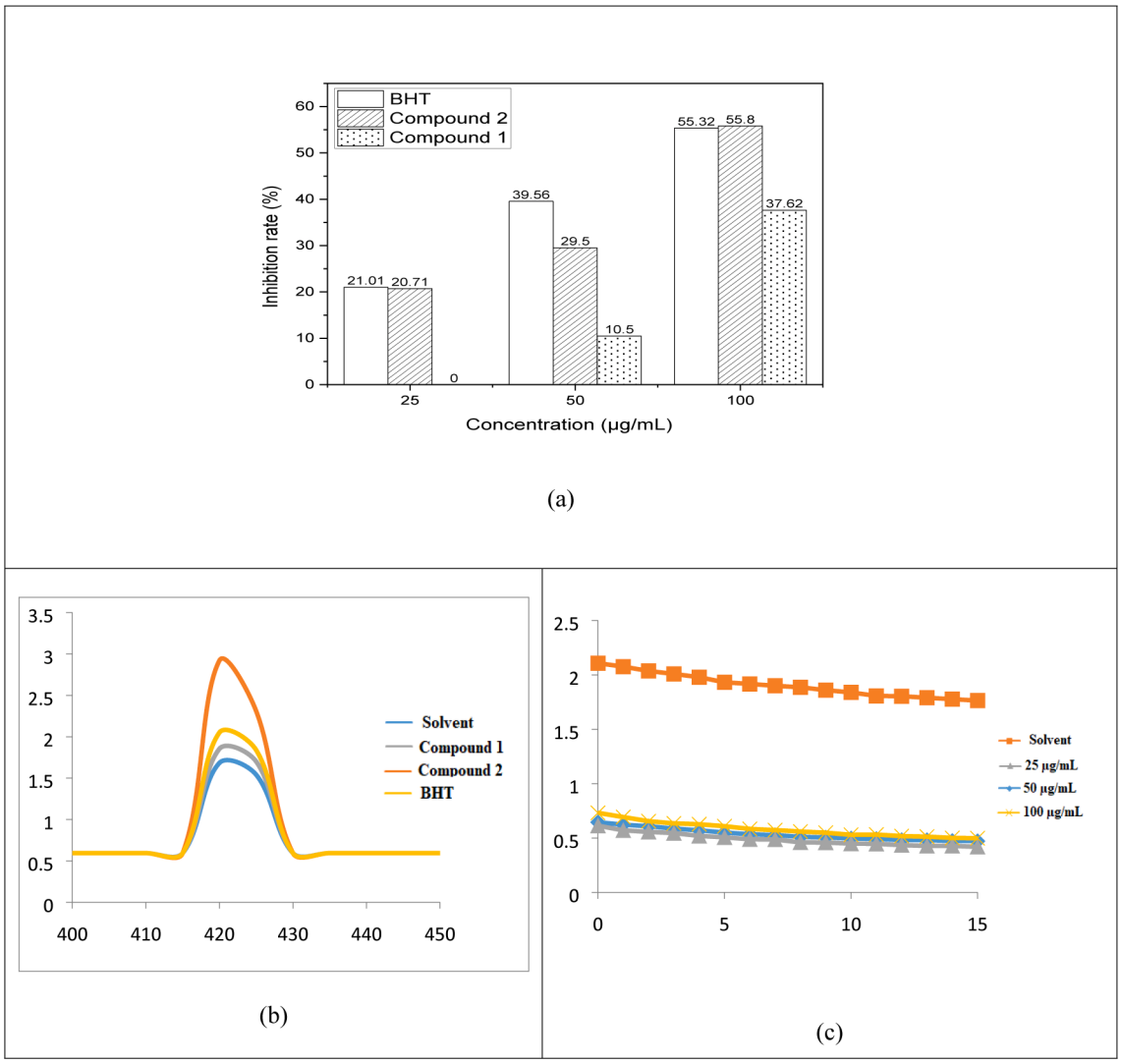

Fig. 3. Hydroxyl radical scavenging Effect of anthraquinone derivatives (a), Fluorescence spectra of (100 µg/mL) upon excitation at 422 nm at solvent, compound 1, 2, and BHT(b), and OH radical kinetic study (c).

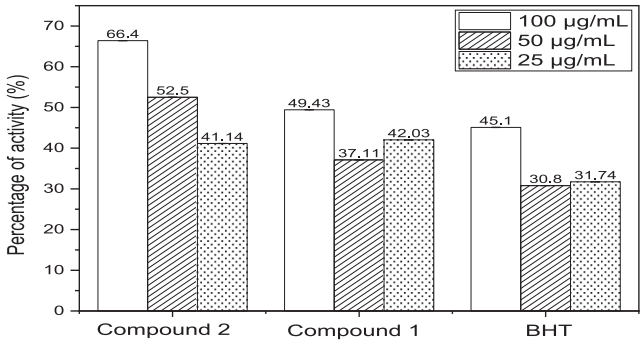

Fig. 4. Hydrogen peroxide radical scavenging Effect of anthraquinone derivative.

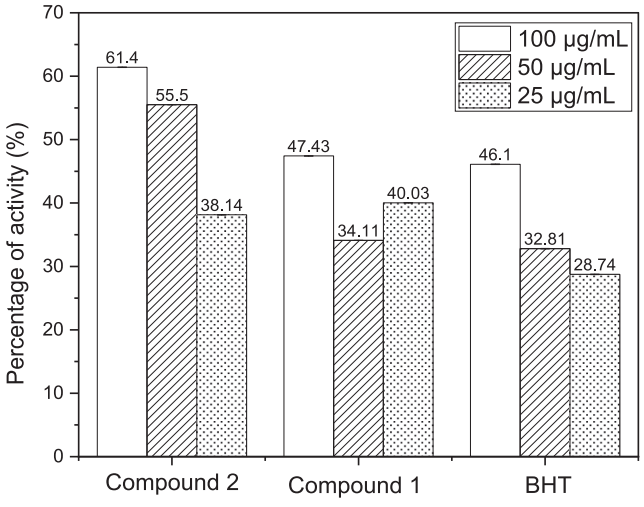

Fig. 5. Nitric oxide scavenging Effect of anthraquinone derivatives.

3.2. DPPH radical scavenging activity

The antioxidants were successful in converting the stable radical DPPH into the yellow-colored diphenyl-picrylhydrazine, as shown by the DPPH experiment's findings. This method, which involves reducing DPPH in an alcoholic solution with an antioxidant that donates

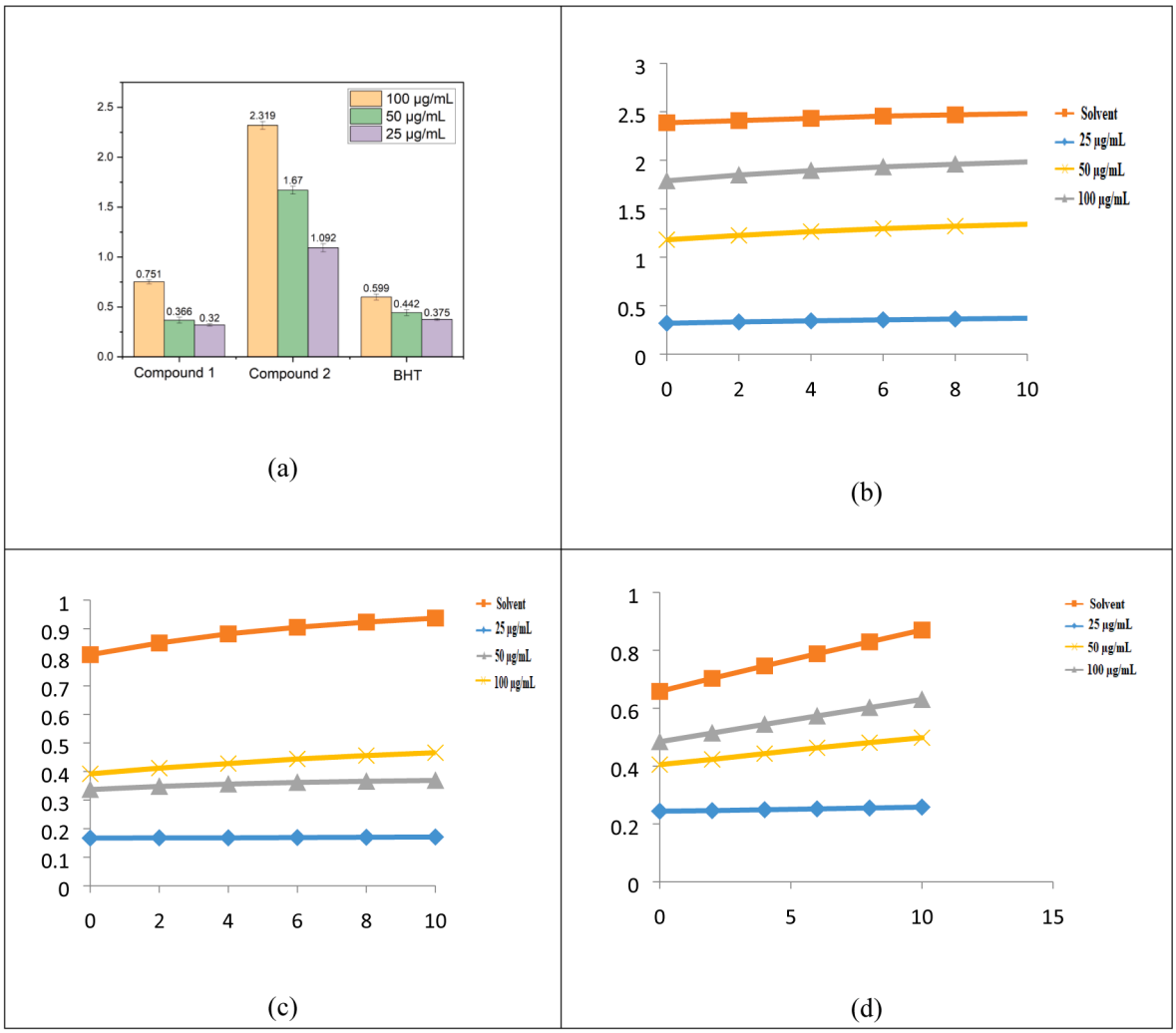

Fig. 6. FRAP activity of reducing power of compounds **1, 2,** and **BHT** (a), compound **1** rate of reaction against FRAP (b), compound **2** rate of kinetic behaviours against FRAP (c), and BHT kinetic behaviours against FRAP (d).

hydrogen throughout the reaction, is based on the creation of the non-radical form DPPH-H during the reaction, mechanism of action shows in scheme 2. When evaluating the level of free radical scavenging activity that antioxidants possess, the reagent DPPH is frequently used. At the same concentration (100 µg/mL), **compounds 1**, **2**, and BHT demonstrated 64.4 %, 46.48 %, and 42.01 % DPPH radical scavenging activity, correspondingly, it is shows that Fig. 2a. According to the results of, the action of the DPPH radical scavenger of BHT stood comparable to that of **compound 1** and **2**, but significantly the **compound 2** was highly active against the **compound 1** and standard **BHT**. The synthesized **compounds 1, 2,** and BHT were also assessed with respect to their antioxidant activities using diphenyl-picrylhydrazinea stable species of free radicals that is frequently employed toward research the antioxidants' capacity to scavenge free radicals. The results of these evaluations may be found in the following sentence: At the beginning, the stability of diphenyl-picrylhydrazine solutions that contained **compounds 1, 2,** and **BHT** was investigated by keeping the solutions in the dark at 25 °C and measuring the absorbance at regular intervals. The presence of **compounds1, 2,** and **BHT** were required to be able to determine radical scavenging by the DPPH capabilities of an anthraquinone derivative. Absorbance dropped quickly (within 5 min) in response to the presence of these compounds. Fig. 2b, c & d shows that kinetic behaviour of reaction rate between the **compounds 1, 2,** and BHT compounds.

3.3. OH· Scavenging activity

At a wavelength of 305 nm for excitation and 407 nm for emission, the fluorescence was measured. Usually, the presence of an antioxidant in the medium causes this fluorescence to diminish. By supplying a hydrogen atom, antioxidant molecules prevent benzoic acid from being hydroxylated.

That is conclude that all chemicals have a concentration-dependent improvement in their ability to scavenge OH radicals. When compared to BHT (55.8 %), **compounds 2** and **1** demonstrated that 55.32 % and 39.56 % at100 µg/mL) shown in Fig. 3a.

The antioxidant activities of the synthesised **compounds 1** and **2** were evaluated using BHT, a stable free radical species that is frequently used to examine the capacity of antioxidants to neutralise free radicals. Beginning with holding BHT solutions containing **compounds 1** and **2** at 25 °C in the dark while occasionally measuring absorbances, the stabilities of these solutions were examined. Since absorbance's decreased quickly, the presence of **compounds 1** and **2** were required to ascertain the OH radical scavenging abilities of anthraquinone derivatives (within 5 min) (Fig. 3b). Kinetic behavior of **compounds 1** and **2** were checked by UV– visible spectroscopy with various concentration, the performance of result shows that Fig. 3c.

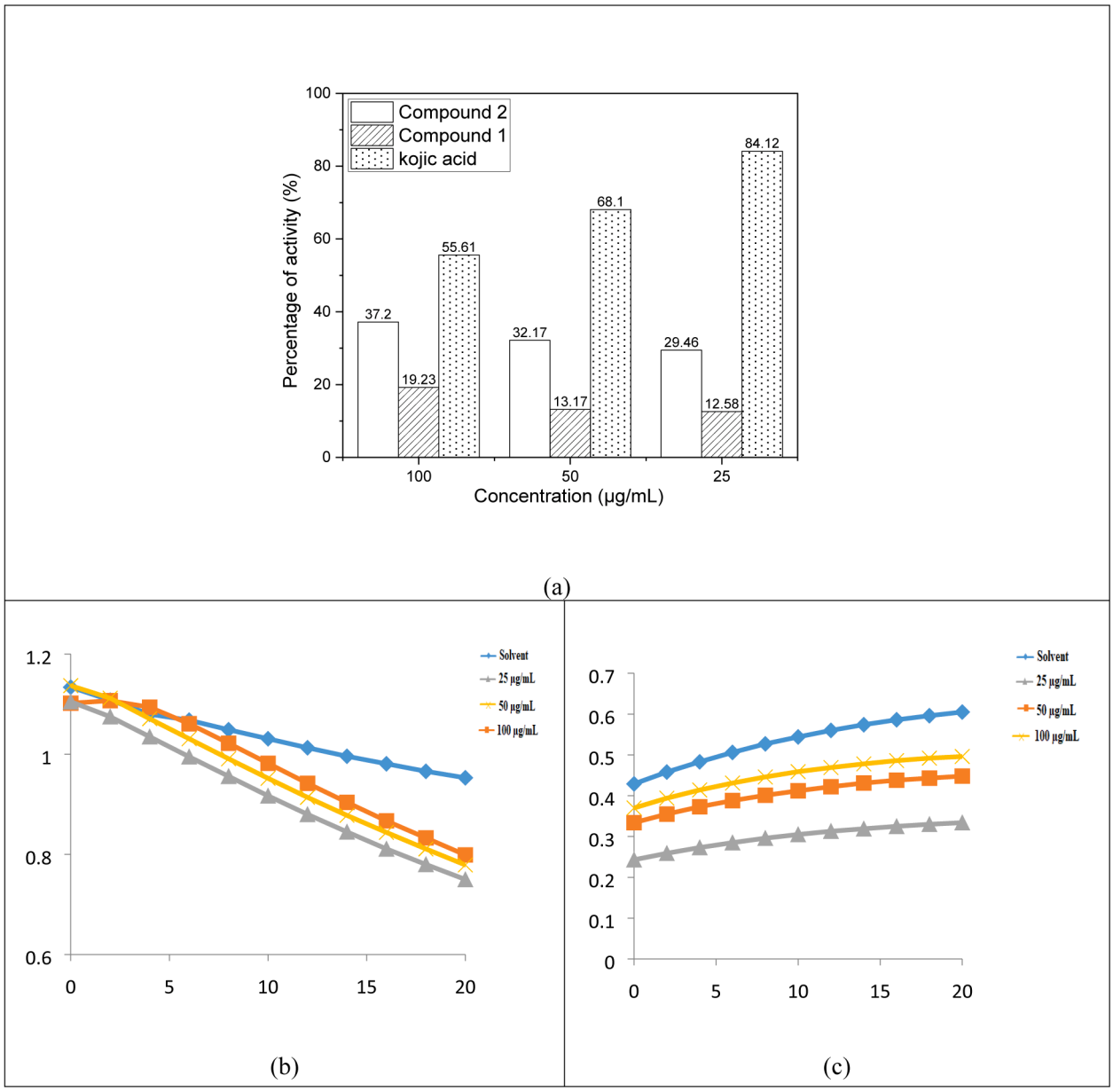

Fig. 7. Tyrosinase activity of compounds **1** and **2** (a), Progress curve for L-Dopa oxidation by mushroom tyrosinase with compound **1** (b), and Progress curve for the oxidation of L-Dopa by mushroom tyrosinase with compound **2**(c).

3.4. H_2O_2 Scavenging activity

By oxidizing abilities of hydrogen peroxide (H_2O_2) are strong. Several oxidizing enzymes, including superoxide dismutase, are capable of forming it in living things. It can move across membranes and has the ability to gently oxidize a variety of substances. In Fig. 4, the capacity for BHT hydrogen peroxide was scavenged demonstrated and contrasted with that **compounds 1** and **2**. The activity of **BHT** was decided to scavenge hydrogen peroxide be 45.1 % at 100 µg/mL. Contrarily, **compounds 1** and **2** shows that the percentage of activity at 50.23 % and 67.03 %, correspondingly, hydrogen peroxide (H_2O_2) scavenging activity. **Compound 2** declined more than **compound 1** at all concentrations, followed by BHT in terms of its ability to scavenge hydrogen peroxide. Transient OH that depends on metal ions radicals can cause DNA oxidative damage when $H_2O_2$is added to cells in culture. Several cell types appear to be less cytotoxic when hydrogen peroxide concentrations are at or below 20–50 mg. As a result, eliminating hydrogen peroxide is crucial for safeguarding the food and drug industries.

3.5. The NO• scavenging activity

NO• with Griess reagent interaction results in formazan, which is detectable spectrophotometrically. The extremely electronegative, somewhat unstable NO• radical quickly receives an electron from another radical. **Compound 2** percent NO• Griess reagent radical inhibition by **compound 2** was 61.4 %, 55.5 %, and 38.14 % at concentrations of 100 µg/mL, 50 µg/mL, and 25 µg/mL, respectively. Compound **2** showed highly increased activity (61.4 %) as compared with BHT (46.1 %) at 100 µg/mL. NO scavenging results are shown in Fig. 5.

3.6. Reducing power

A compound's lowering capability can be an important predictor of its possible action. When compared to the standards, **compounds 1** and **2** demonstrated efficient decreasing force when employing the $K_4[Fe(CN)_6].3H_2O$ reduction method, as shown in Fig. 6a. The Fe^{3+}-Fe^{2+}

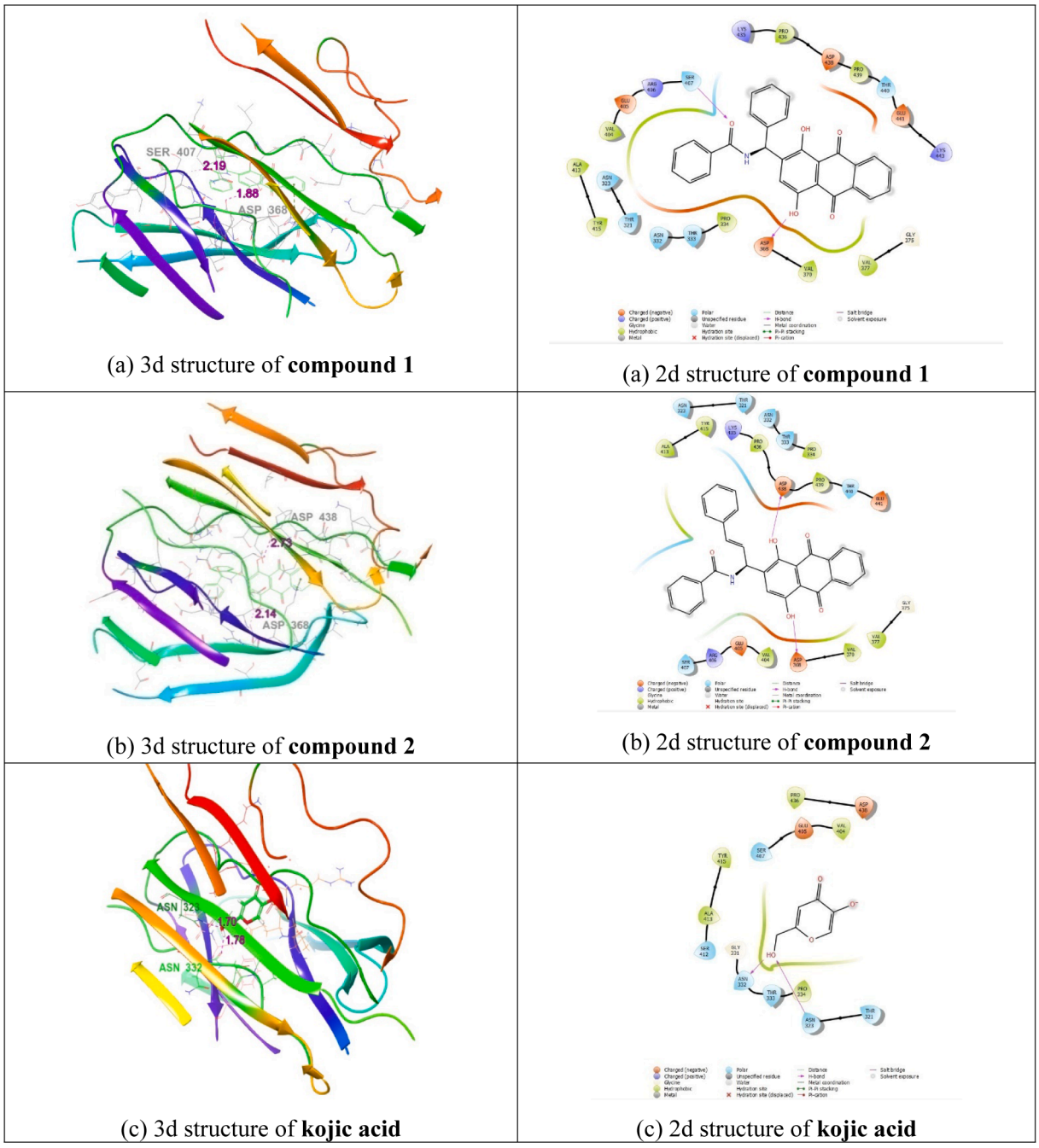

Fig. 8. (a) Molecular docking study of Compound 1, (b) Compound 2, and (c) Kojic acid with 2Y9X protein (2d and 3d interaction structures).

Table 1
Docked result of Compounds with **2Y9X** using XP method.

S. No	Compound/ Drug	Dock Score	Interacting residues	Bond Length
1.	Compound **1**	−2.7	Asp 368, Ser 407	1.88, 2.19
2.	Compound **2**	−1.7	Asp 368, Asp 438	2.14, 2.73
3.	Kojic acid	−4.7	Asn 323, Asn 332	1.70, 1.78

transition was examined used as Oyaizu method to assess the reductive ability of **compounds 1** and **2**. **Compounds1** and **2** displayed powerful reducing activity at various doses (100–25 μg/mL). **Compounds 1** and **2** had the greatest reducing power, followed by typical compounds in the following order: **Compound2** > **Compound1** > BHT. The results show that **compound 2** has electron donor capabilities that allow it to neutralize free radicals by producing stable products. *In vivo,* the reducing process terminates potentially hazardous radical chain reactions. Compared to Wang and Yang's results, this test's **compound 1** absorbance is lower. As a result of the spectrophotometers, that was achievable, and agents utilized in the two experiments were different, resulting in different results.

In acidic media, the Fluorescence recovery after photobleaching assay assesses antioxidants' ability to decrease the complex $[Fe^{3+}\text{-}(TPTZ)_2]^{3+}$ to the brightly blue complex $[Fe^{2+}\text{-}(TPTZ)_2]^{2+}$. The absorbance rise at 593 nm is measured, and compared to Fe^{2+} ion standard or a conventional anti-oxidant solution, such as BHT, to obtain FRAP values. The most potent reducing ability was detected in BHT (0.599) at concentrations of 100 μg/mL, whereas Cu NPs absorbed relatively poor reducing abilities at concentrations ranging from 25 to 100 μg/mL when

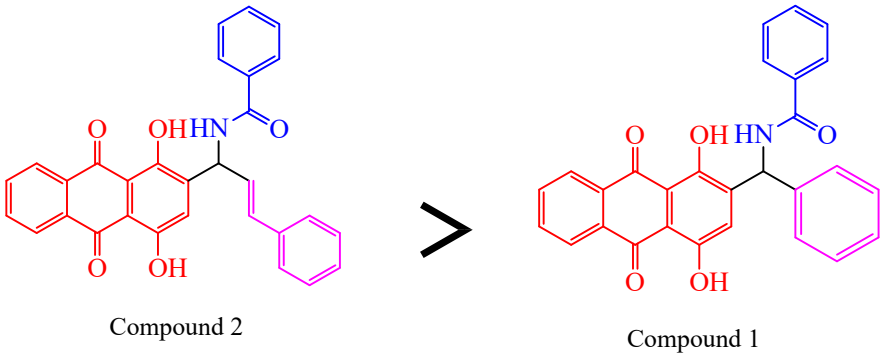

Comparision of **compound 1**, and **2**

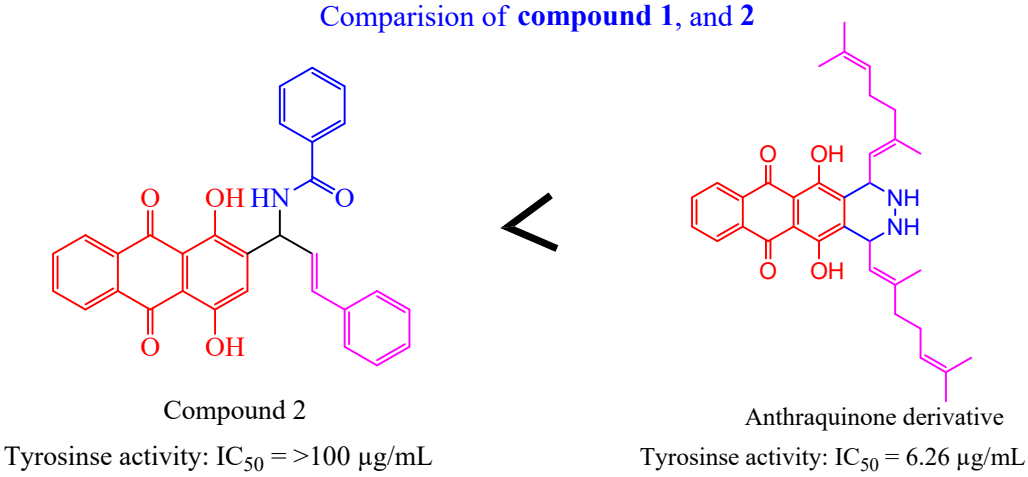

Anti-tyrosinase activity

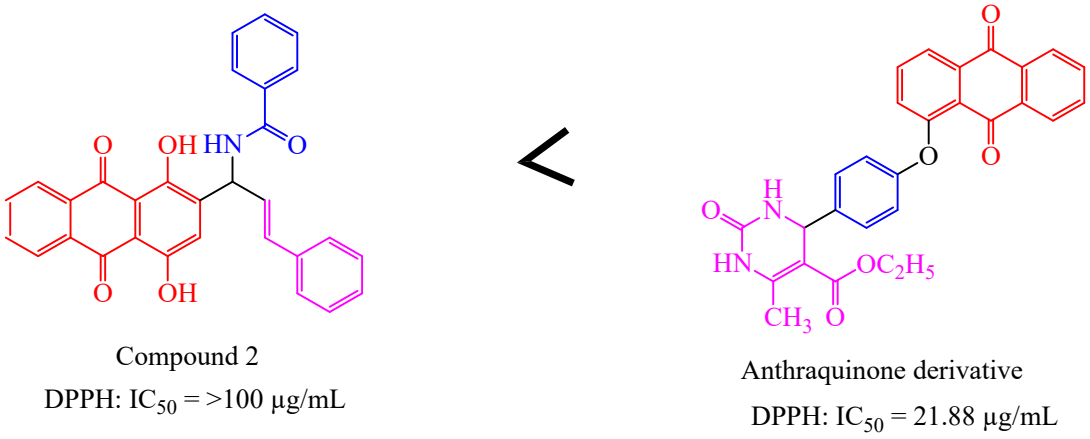

Antioxidant activity

Fig. 9. Structural activity relationship.

compared with BHT. Fig. 6b shows that different concentrations of the Fe^{3+}-Fe^{2+} reductive potential in **compound 1** kinetics (25–100 µg/mL)-FRAP-FRAP. Fig. 6c shows that various concentrations of the Fe^{3+}-Fe^{2+} reductive potential (FRAP) (25–100 µg/mL) in **compound 2** kinetics. Fig. 6d shows thatdifferent amounts of reductive potential (25–100 µg/mL) affect the BHT kinetics of Fe^{3+}, Fe^{2+}, and FRAP.

3.7. Anti-tyrosinase activity

Fig. 7a illustrates these findings, which showed that the extract's tyrosinase inhibitory effect was reversible and more potent than blocking the enzyme through binding. The extracts that bind the copper in the enzyme's active site consequently display competitive inhibition that is comparable to Kojic acid. The L-Dopa oxidation progression curve, as mediated by mushroom tyrosinase, is shown in Fig. 7b & c. All values were average ± SD of five values. Reported average values for all parameters within a column with same superscripts are not significantly different ($P > 0.05$).

3.8. Molecular docking

3.8.1. Ligand preparation

Chem 3D pro and Chem draw 12.0 were used to draw the ligands (**Compound 1**, **2**, and Kojic acid). For use in docking investigations, the

ligand molecules were then transformed into a Protein Data Bank (PDB) file.

3.8.2. Receptor preparation

The protein data bank was used to download this structure, which represents a protein that binds mosquito odorant. Water molecules and ligands are taken out of the utilising Discovery Studio 2019 as a receptor. The SWISS PDB Viewer was used to lower the energy of the receptor. After that, the receptor underwent molecular docking.

3.8.3. Identification of binding pocket

The Discovery Studio 2019 application and a co-crystallized ligand were used to examine the target protein's binding pocket. Asp 368, Asp 438, Asp 368, Ser 407, Asn 323, and Asn 332 residues were found in the binding pocket.

3.8.4. Docking

In order to investigate the interactions between **compounds 1**, **2**, and kojic acid, the mosquito odorant binding protein, molecular docking experiments were carried out using Schrodinger Maestro 9.2. The amino acid residues that made up the binding pocket were taken into account when choosing the docking grid boxes. With an exhaustiveness score of 8, the interactions were visually inspected in the PyMOL and Discovery Studio programmes. The software utilized to analyze the docking behaviour of **compounds 1, 2,** and kojic acid with 2Y9X protein is 9.2 for the Schrodinger Maestro. A 2D illustration of a molecule coupled with a receptor for **compounds 1** and **2** comparatively, the binding affinity of **compound 2** for the 2Y9X protein is substantially lower (-1.7 kcal/mol) than that of kojic acid (-4.7 kcal/mol). Kojic acid was employed as a benchmark because it is a widely available insecticide for controlling mosquitoes.

The stability of protein–ligand interaction is greatly influenced by the hydrogen bond, and the ideal distance amongst the H-acceptor and H-donor atoms is lower than 3.5. In **compounds 1** and **2** having strong hydrogen connections to the corresponding 2Y9X proteins, hydrogen bond lengths of less than 3.5 were discovered. **Compound 2** created hydrogen-bond interactions with receptor 2Y9X. The hydrogen-interacting residues Asp 368 and Asp 438 have a bond length of 2.14 and 2.73, respectively. VAL 370, GLY 375, VAL 377, VAL 404, GLU 405, ARG 406, SER 407, ALA 413, TYR 415, LYS 435, PRO 436, ASP 438, and PRO 439 are among the amino acid residues. According to Fig. 8a, the receptor's docking score (-1.7 kcal/mol) and a 3D representation of the inhibitor molecule were implicated in hydrophobic interactions. **Compound 2** is more active than **compound 1** and kojic acid. As a result, the complex of Asp 368 and Ser 407, which has a bond length of 1.88, 219, is an interacting residue that interacts with hydrogen. LYS 435, PRO 436, ASP 438, PRO 439, THR 440, GLU 441, and LYS 443 The amino acid residues are THR 321, ASN 323, ASN 332, THR 333, PRO 334, ASP 368, VAL 370, GLY 375, VAL 377, VAL 404, ARG 406, SER 407, ALA 413, and TYR 415. Inhibitor molecules docked into receptors were depicted in 3D in Fig. 8b, and their hydrophobic contacts were indicated by their docking score (-2.7 kcal/mol).

As a result, the Asn 323, Asn 332, of kojic acid, which has a bond length of 1.70, 1.78, is an interfering residue that interacts with hydrogen. THR 321, ASN 323, GLY 331, ASN 332, THR 333, PRO 334, VAL 404, GLU 405, SER 407, SER 412, ALA 413, TYR 415, ASP 438, and PRO 436 are among the amino acid residues. Inhibitor molecules docked into receptors were depicted in 3D in Fig. 8c, and their hydrophobic contacts were indicated by their docking score (-4.7 kcal/mol). Table 1 shows that docking socre, interacting the residues between the compounds with2Y9X proteins (Akbar et al., 2022).

3.8.5. Structure–activity relationship (SAR) analysis

The correlation between the biological activities of physiologically significant substances and their chemical composition in the test system is referred to as the structural-activity relationship (SAR). We discovered a number of critical factors while analysing the relationships between structure and activity.

Fig. 9 illustrate the SAR of **compound 1** and **2**. The **compound 2** was highly active against all other activities compared with standard and compound **1**.

Compound 2, which has anthraquinone connected with benzamide and benzaldehyde, it is highly active against all the activity, but lowly active against previously reported anthraquinone derivative (Selvaraj et al., 2020) was highly active (IC_{50} = 6.26 μg/mL) against anti-tyrosinase activity.

Compound 2, which has anthraquinone connected with benzamide and benzaldehyde, it is highly active against all the activity, but lowly active against previously reported anthraquinone derivative (Zarren et al., 2021) was highly active (IC_{50} = 21.88 μg/mL) against antioxidant activity (DPPH).

Furthermore study is required since lead **compound 2** constitute the novel class of very effective antioxidant, and anti-tyrosinase.

4. Conclusion

According to the results of the present investigation, anthraquinone derivatives **compounds 1** and **2** were found to be a potent antioxidant and anti-tyrosinase in several *in vitro* tests, including reducing power, DPPH radicals, hydroxyl radicals, H_2O_2, and NO radical scavenging in comparison to the typical antioxidant chemical BHT. **Compound 2** binding energy is higher than that of ordinary kojic acid in the molecular docking investigation when compared to **compounds 1** and **2**. Based on the aforementioned findings, it can be used to maintain nutritional quality, extend the shelf life of food and medicine, delay the development of hazardous oxidation products, and minimise or stop the oxidation of lipids in dietary items.

Declaration of Competing Interest

The authors declare that they have no known competing financial interests or personal relationships that could have appeared to influence the work reported in this paper.

Acknowledgments

Authors are thankful to the Researchers Supporting Project number (RSPD2023R728), King Saud University, Riyadh, Saudi Arabia.

Appendix A. Supplementary data

Supplementary data to this article can be found online at https://doi.org/10.1016/j.jksus.2023.102971.

References

Akbar, I., Radhakrishnan, S., Meenakshi sundaram, K., Manilal, A., Hatamleh, A. A., Alnafisi, B. K.,& Balasubramani, R., 2022. Design of 1, 4-Dihydropyridine Hybrid Benzamide Derivatives: Synthesis and Evaluation of Analgesic Activity and Their Molecular Docking Studies. Drug Design, Development and Therapy, 4021-4039.

Assefa, A.D., Keum, Y.S., Saini, R.K., 2018. A comprehensive study of polyphenols contents and antioxidant potential of 39 widely used spices and food condiments. J. Food Meas. Charact. 12, 1548–1555. https://doi.org/10.1007/s11694-018-9770-z.

Benzie, I.F., Devaki, M., 2018. The ferric reducing/antioxidant power (FRAP) assay for non-enzymatic antioxidant capacity: concepts, procedures, limitations and applications. Measurement of Antioxidant Activity & Capacity: Recent Trends and Applications 77–106. https://doi.org/10.1002/9781119135388.ch5.

Berretta, A.A., Silveira, M.A.D., Capcha, J.M.C., De Jong, D., 2020. Propolis and its potential against SARS-CoV-2 infection mechanisms and COVID-19 disease: Running title: Propolis against SARS-CoV-2 infection and COVID-19. Biomed. Pharmacother. 131, 110622 https://doi.org/10.1016/j.biopha.2020.110622.

Chidambaram, S., El-Sheikh, M.A., Alfarhan, A.H., Radhakrishnan, S., Akbar, I., 2021. Synthesis of novel coumarin analogues: Investigation of molecular docking interaction of SARS-CoV-2 proteins with natural and synthetic coumarin analogues and their pharmacokinetics studies. Saudi Journal of Biological Sciences 28 (1), 1100–1108. https://doi.org/10.1016/j.sjbs.2020.11.038.

Chighizola, C.B., Andreoli, L., Gerosa, M., Tincani, A., Ruffatti, A., Meroni, P.L., 2018. The treatment of anti-phospholipid syndrome: a comprehensive clinical approach. J. Autoimmun. 90, 1–27. https://doi.org/10.1016/j.jaut.2018.02.003.

Cicek, S.S., Ugolini, T., Girreser, U., 2019. Two-dimensional qNMR of anthraquinones in Frangulaalnus(Rhamnusfrangula) using surrogate standards and delay time adaption. AnalyticaChimicaActa 1081, 131–137. https://doi.org/10.1016/j.aca.2019.06.046.

Dehnavi, S., Kiani, A., Sadeghi, M., Biregani, A.F., Banach, M., Atkin, S.L., Sahebkar, A., 2021. Targeting AMPK by statins: a potential therapeutic approach. Drugs 81 (8), 923–933. https://doi.org/10.1007/s40265-021-01510-4.

Diep, T.T., Rush, E.C., Yoo, M.J.Y., 2022. Tamarillo (Solanumbetaceum Cav.): A review of physicochemical and bioactive properties and potential applications. Food Rev. Intl. 38 (7), 1343–1367. https://doi.org/10.1080/87559129.2020.1804931.

Duval, J., Pecher, V., Poujol, M., Lesellier, E., 2016. Research advances for the extraction, analysis and uses of anthraquinones: A review. Ind. Crop. Prod. 94, 812–833. https://doi.org/10.1016/j.indcrop.2016.09.056.

Feilcke, R., Arnouk, G., Raphane, B., Richard, K., Tietjen, I., Andrae-Marobela, K., Frolov, A., 2019. Biological activity and stability analyses of knipholoneanthrone, a phenyl anthraquinone derivative isolated from KniphofiafoliosaHochst. J. Pharm. Biomed. Anal. 174, 277–285. https://doi.org/10.1016/j.jpba.2019.05.065.

Friščić, M., ŠtibrićBaglama, M., Milović, M., HazlerPilepić, K., Maleš, Ž., 2018. Content of bioactive constituents and antioxidant potential of Galium L. species. Croatica Chemica Acta 91 (3), 411–417. https://doi.org/10.5562/cca3379.

Garcia-Caparros, P., De Filippis, L., Gul, A., Hasanuzzaman, M., Ozturk, M., Altay, V., Lao, M.T., 2021. Oxidative stress and antioxidant metabolism under adverse environmental conditions: a review. Bot. Rev. 87, 421–466. https://doi.org/10.1007/s12229-020-09231-1.

Gecibesler, I.H., Disli, F., Bayindir, S., Toprak, M., Tufekci, A.R., Yaglıoglu, A.S., Adem, S., 2021. The isolation of secondary metabolites from Rheum ribes L. and the synthesis of new semi-synthetic anthraquinones: Isolation, synthesis and biological activity. Food Chem. 342, 128378 https://doi.org/10.1016/j.foodchem.2020.128378.

Ghosh, A., Tiwari, G.J., 2018. Role of nitric oxide-scavenging activity of Karanjin and Pongapin in the treatment of Psoriasis. 3. Biotech 8 (8), 338. https://doi.org/10.1007/s13205-018-1337-5.

Ighodaro, O.M., Akinloye, O.A., 2018. First line defence antioxidants-superoxide dismutase (SOD), catalase (CAT) and glutathione peroxidase (GPX): Their fundamental role in the entire antioxidant defence grid. Alexandria Journal of Medicine 54 (4), 287–293. https://doi.org/10.1016/j.ajme.2017.09.001.

Juan, C.A., Pérez de la Lastra, J.M., Plou, F.J., Pérez-Lebeña, E., 2021. The chemistry of reactive oxygen species (ROS) revisited: outlining their role in biological macromolecules (DNA, lipids and proteins) and induced pathologies. Int. J. Mol. Sci. 22 (9), 4642. https://doi.org/10.3390/ijms22094642.

Kammona, O., Kiparissides, C., 2020. Recent advances in antigen-specific immunotherapies for the treatment of multiple sclerosis. Brain Sci. 10 (6), 333. https://doi.org/10.3390/brainsci10060333.

Karim, M.A., Islam, M.A., Islam, M.M., Rahman, M.S., Sultana, S., Biswas, S., Hasan, M. N., 2020. Evaluation of antioxidant, anti-hemolytic, cytotoxic effects and anti-bacterial activity of selected mangrove plants (Bruguieragymnorrhiza and Heritieralittoralis) in Bangladesh. Clinical Phytoscience 6 (1), 1–12. https://doi.org/10.1186/s40816-020-0152-9.

Korkmaz, N., Dayangaç, A., Sevindik, M., 2021. Antioxidant, antimicrobial and antiproliferative activities of Galium aparine. Journal of Faculty of Pharmacy of Ankara University 45 (3), 554–564. https://doi.org/10.33483/jfpau.977776.

Kumar, R.S., Moydeen, M., Al-Deyab, S.S., Manilal, A., Idhayadhulla, A., 2017. Synthesis of new morpholine-connected pyrazolidine derivatives and their antimicrobial, antioxidant, and cytotoxic activities. Bioorg. Med. Chem. Lett. 27 (1), 66–71. https://doi.org/10.1016/j.bmcl.2016.11.032.

Lateef, A., Ojo, S.A., Elegbede, J.A., Azeez, M.A., Yekeen, T.A., Akinboro, A., 2017. Evaluation of some biosynthesized silver nanoparticles for biomedical applications: hydrogen peroxide scavenging, anticoagulant and thrombolytic activities. J. Clust. Sci. 28, 1379–1392. https://doi.org/10.1007/s10876-016-1146-0.

Maher, P.A., 2020. Focus: Plant-based Medicine and Pharmacology: Using Plants as a Source of Potential Therapeutics for the Treatment of Alzheimer's Disease. Yale J. Biol. Med. 93 (2), 365.

Malik, M.S., Alsantali, R.I., Jassas, R.S., Alsimaree, A.A., Syed, R., Alsharif, M.A., Ahmed, S.A., 2021. Journey of anthraquinones as anticancer agents–a systematic review of recent literature. RSC Adv. 11 (57), 35806–35827. https://doi.org/10.1039/D1RA05686G.

Malik, E.M., Müller, C.E., 2016. Anthraquinones as pharmacological tools and drugs. Med. Res. Rev. 36 (4), 705–748. https://doi.org/10.1002/med.21391.

Martorell, M., Castro, N., Victoriano, M., Capó, X., Tejada, S., Vitalini, S., Sureda, A., 2021. An update of anthraquinone derivatives emodin, diacerein, and catenarin in diabetes. Evid. Based Complement. Alternat. Med.Ecam 2021. https://doi.org/10.1155/2021/3313419.

Masi, M., Evidente, A., 2020. Fungal Bioactive Anthraquinones and Analogues. Toxins 12 (11), 714. https://doi.org/10.3390/toxins12110714.

Mohamadzadeh, M., Zarei, M., Vessal, M., 2020. Synthesis, in vitro biological evaluation and in silicomolecular docking studies of novel β-lactam-anthraquinone hybrids. Bioorg. Chem. 95, 103515 https://doi.org/10.1016/j.bioorg.2019.103515.

Özmatara, M.B., 2020. Phytosynthesis of Iron Nanoparticles using Galium Aparine L. Extract: their Characterization and Antioxidant Activity. Sigma Journal of Engineering and Natural Sciences 38 (4), 2169–2176.

Rastogi, V., Tomar, J., Patni, T., Vijay, C., Sharma, P., 2019. Anti-tubercular minimum inhibitory concentration (MIC) and chemical characterization of ethnobotanical mixture used in the treatment of tuberculosis. Indian J Microbiol Res 6 (1), 50–56. https://doi.org/10.18231/2394-5478.2019.0011.

Selvaraj, K., Daoud, A., Alarifi, S., Idhayadhulla, A., 2020. Tel-Cu-NPs catalyst: Synthesis of naphtho [2, 3-g] phthalazine derivatives as potential inhibiters of tyrosinase enzymes and their investigation in kinetic, molecular docking, and cytotoxicity studies. Catalysts 10 (12), 1442. https://doi.org/10.3390/catal10121442.

Siddamurthi, S., Gutti, G., Jana, S., Kumar, A., Singh, S.K., 2020. Anthraquinone: a promising scaffold for the discovery and development of therapeutic agents in cancer therapy. Future Med. Chem. 12 (11), 1037–1069. https://doi.org/10.4155/fmc-2019-0198.

Tian, W., Wang, C., Li, D., Hou, H., 2020. Novel anthraquinone compounds as anticancer agents and their potential mechanism. Future Med. Chem. 12 (7), 627–644. https://doi.org/10.4155/fmc-2019-032.

Tikhomirov, A.S., Shtil, A.A., Shchekotikhin, A.E., 2018. Advances in the discovery of anthraquinone-based anticancer agents. Recent Pat. Anticancer Drug Discov. 13 (2), 159–183. https://doi.org/10.2174/1574892813666171206123114.

Vitale, G.A., Coppola, D., Palma Esposito, F., Buonocore, C., Ausuri, J., Tortorella, E., de Pascale, D., 2020. Antioxidant molecules from marine fungi: Methodologies and perspectives. Antioxidants 9 (12), 1183. https://doi.org/10.3390/antiox9121183.

Wang, L., Li, B., Dionysiou, D.D., Chen, B., Yang, J., Li, J., 2022a. Overlooked formation of H2O2 during the hydroxyl radical-scavenging process when using alcohols as scavengers. Environ. Sci. Tech. 56 (6), 3386–3396. https://doi.org/10.1021/acs.est.1c03796.

Wang, L., Wang, N., Zhang, W., Cheng, X., Yan, Z., Shao, G., Fu, C., 2022b. Therapeutic peptides: Current applications and future directions. Signal Transduct. Target. Ther. 7 (1), 48. https://doi.org/10.1038/s41392-022-00904-4.

Zarren, G., Shafiq, N., Arshad, U., Rafiq, N., Parveen, S., Ahmad, Z., 2021. Copper-catalyzed one-pot relay synthesis of anthraquinone based pyrimidine derivative as a probe for antioxidant and antidiabetic activity. J. Mol. Struct. 1227, 129668 https://doi.org/10.1016/j.molstruc.2020.129668.